Hydrophilic patterning of superhydrophobic surfaces by atmospheric-pressure plasma jet

Faze Chen[1], Wenji Xu[1], Yao Lu[2], Jinlong Song[1], Shuai Huang[1], Long Wang[1], Ivan P. Parkin[2], Xin Liu[1]

[1]*Key Laboratory for Precision and Non-Traditional Machining Technology of Ministry of Education, Dalian University of Technology, Dalian 116024, People's Republic of China*
[2]*Department of Chemistry, Materials Chemistry Research Centre, University College London, 20 Gordon Street, London, WC1H OAJ, United Kingdom*
E-mail: xinliu@dlut.edu.cn

Published in Micro & Nano Letters; Received on 19th October 2014; Revised on 26th November 2014; Accepted on 3rd December 2014

An atmospheric-pressure plasma jet (APPJ) has been developed to fabricate hydrophilic patterns on superhydrophobic surfaces. The surface morphologies, chemical compositions and wettability were investigated using scanning electron microscopy, Fourier-transform infrared spectrophotometry, X-ray photoelectron spectroscopy and water contact angle measurement. The results show that the superhydrophobic areas exposed to the APPJ could be completely converted to superhydrophilic without changing the macro and microsurface morphologies. The transition from superhydrophobicity to superhydrophilicity is because of the decrease of hydrophobic fluorine-containing functional groups and the increase of the hydrophilic oxygen-containing functional groups. Combined with scanning and mask technology, complex and large-area wettability contrast patterns can be easily fabricated on various superhydrophobic substrates by the APPJ treatment. Additionally, the retention of intrinsic microstructures enables the surface to recover superhydrophobicity only by using surface fluorination. This results in a rapid reversible transition between superhydrophilicity and superhydrophobicity.

1. Introduction: Smart materials have attracted worldwide attention because of their various applications such as emerging forward osmosis [1], sensors [2] and surface patterning. In particular, patterned surfaces with large wettability contrast are of great importance in practical applications such as open channel microfluidics, water harvesting, condensation, droplet guided transport, lab-on-a-chip systems and offset printing [3–10]. Several methods to prepare wettability contrast patterns have been reported, including the selective ultraviolet (UV) degradation of photocatalytic coatings [10–14], laser irradiation [15], inkjet printing [16], the adhesive tape method [17] and the soft lithography process [18, 19]. In the aforementioned methods, UV radiation combined with a photomask is the most popular and effective method, which can fabricate complex wettability contrast patterns. However, UV radiation is only effective for some photocatalytic materials, for example TiO_2, V_2O_5, ZnO and so on, and mostly regarding microfabrications [20, 21]. In addition, such photocatalytic materials are easily degraded in some cases even if they are coated on other substrates. Thus, it is necessary to develop a new and facile method that can fabricate large-area and complex wettability contrast patterns directly on various superhydrophobic substrates.

In recent years, low-pressure plasma treatment has shown application potential in the fabrication of wettability contrast patterns and wide-range control of surface wettability [6, 18, 22, 23]. However, the low-pressure conditions require expensive vacuum equipment which also significantly limits the treated sample size, the processing efficiency and large-scale industrial utilisation. West *et al.* [24] obtained hydrophilic patterns on a hydrophobic glass substrate via a dielectric barrier discharge (DBD) helium (He) microplasma jet. However, according to the study of Xian *et al.* [25], when metal contacted with an electrically driven DBD He plasma jet, it would affect the discharge and would have effects on the intensity of the plasma jet, which was totally different from a gas-driven bare electrode discharge N_2 plasma jet. Therefore, the method proposed by West *et al.* was confined to the pattern fabrication on non-metallic substrates since electrical breakdown or arc discharge occurs, which damages the surface microstructure when in contact with metals or semiconductors. For these reasons, there are demands for methods to switch wettability on metal surfaces at atmospheric pressure for surface patterning and an N_2 plasma jet generated by bare electrode discharge would be an available tool for this purpose. In the work reported in this Letter, a facile atmospheric-pressure plasma jet (APPJ) generated by bare electrode discharge was developed to fabricate hydrophilic patterns on various superhydrophobic surfaces. After APPJ irradiation for only 30 s, the water contact angle (WCA) of exposed regions decreased from 159.3° to $< 10°$, which demonstrates extreme wettability contrast from the initial superhydrophobic regions. This method does not need expensive vacuum equipment and, when combined with scanning and the mask, can quickly and easily fabricate large-area and complex wettability contrast patterns on various superhydrophobic substrates.

2. Experimental: Superhydrophobic metal plates were fabricated by the previous published methods [26–30]. Briefly, polished metal plates were first electrochemically treated to construct the rough structures required for superhydrophobicity. Then, the rough samples were immersed in an ethanol solution of fluoroalkylsilane [FAS, $C_8F_{13}H_4Si(OCH_2CH_3)_3$] for surface fluorination to lower the surface free energy.

The APPJ source used for this study was described previously [31], while the frequency of the AC power supply was adjusted to 60 kHz and the discharge power was nearly 2.50 W for the APPJ treatment. The flow rate of nitrogen (of purity 99.999%) was controlled to be 10 standard litres per minute by a mass flow controller. Once nitrogen was introduced through the source and high voltage was applied, a plasma jet with a diameter of ~4 mm was ejected to the surrounding air.

Hydrophilic patterns were constructed on superhydrophobic metal substrates by selective APPJ exposure using masks to block out plasma exposure in certain areas. Superhydrophobic metal substrates were positioned 10 mm from the nozzle outlet and the APPJ source was moved along the designed tracks at 0.5 mm/s for the fabrication of hydrophilic patterns.

To investigate the relationship between the APPJ treatment time and the WCAs of the surfaces, the as-prepared superhydrophobic

aluminium plates not covered by the mask were treated by non-scanned APPJ for different times, ranging from 1 to 60 s. The superhydrophobic surface was converted into a superhydrophilic one after being radiated by APPJ for 45 s. The recovery of the superhydrophobicity was realised by immersion in the FAS-ethanol solution again. As a result, the wettability transition between superhydrophobicity and superhydrophilicity was realised by the alternation of APPJ treatment and surface fluorination.

The optical emission spectrum (OES) of APPJ downstream was measured by a monochromator (Andor SR-750i) with a grating groove of 1200 lines/mm and glancing wavelength of 500 nm. The surface morphologies of the samples were observed by a scanning electron microscope (JSM-6360LV, Japan). The surface chemistry of the samples was analysed by a Fourier-transform infrared (FTIR) spectrometer (JACSCO, Japan) and X-ray photoelectron spectroscopy (XPS, Thermo ESCALAB 250Xi, USA. Al-Kα radiation and C 1s peak (284.6 eV) reference). WCAs were measured by an optical contact angle meter (Krüss, DSA100, Germany) at room temperature. Water droplets of 5 µL were dropped onto the superhydrophobic areas or APPJ-treated areas and the average WCA values were determined by measuring the same sample at five different positions.

3. Results and discussion: Figs. 1*a* and *d* show the masks with the microchannel and China's eight diagrams for selective exposure to APPJ (black areas in pattern design) that were used for hydrophilic pattern fabrication, while unexposed regions (white areas) remained superhydrophobic. Hence, the surface comprises different wettability domains relating to the superhydrophobic/hydrophilic patterns. The red dotted lines and the arrows in Figs. 1*a* and *d* represent the APPJ motion. The samples were dipped into food colouring after APPJ treatment, and the exposed regions immediately dyed red, as shown in Figs. 1*b* and *e*. Figs. 1*c* and *f* show the close-up of the hydrophilic microchannel and China's eight diagrams patterns, respectively. With APPJ scanning and large-scale APPJ development, large-area wettability contrast pattern fabrication could be easily realised.

Fig. 2*a* shows the SEM images of the unexposed and exposed areas on superhydrophobic aluminium surfaces during APPJ treatment. It clearly shows that the two surfaces were all rather rough and many rectangular-shaped plateaus with a size of a few microns were distributed homogeneously on irregular pits and protrusions, indicating that the APPJ treatment had no significant influence on the surface morphology of the samples. It is well known that the surface wettability is determined by surface morphology and chemical compositions [32], thus the variation in wettability is probably because of the changes in surface chemical composition.

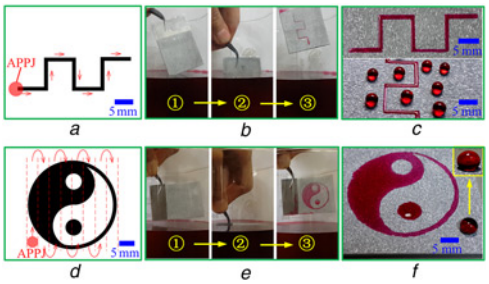

Figure 1 *Hydrophilic patterning of superhydrophobic aluminium surfaces by nitrogen APPJ*
a and *d* Masks used for selective APPJ exposure
Red dotted lines and arrows represent the APPJ pathway
b and *e* APPJ-treated samples were dipped into food colouring and the areas exposed to APPJ were dyed red
c and *f* Photographs of hydrophilic patterns on superhydrophobic aluminium surfaces created by masked APPJ treatments

The surface chemical compositions of the unexposed and exposed areas of the selective APPJ-treated superhydrophobic aluminium surfaces were analysed by FTIR spectrophotometry and XPS, as shown in Figs. 2*b* and *c*, respectively. We can see from Fig. 2*b* that the C–F stretching of $–CF_2$ and $–CF_3$ groups of the FAS molecules between 1242 and 1120 cm^{-1}, which reduced the surface energy effectively, was weakened dramatically under APPJ treatment. It was also notable that the FTIR spectrum for the APPJ-treated areas developed stronger and broader absorption bands around 3435 cm^{-1}, corresponding to –OH stretching vibrations. Bands corresponding to –CO and –COO around 1650 and 1548 cm^{-1} were also more apparent after APPJ treatment. The XPS analysis depicted in Fig. 2*c* demonstrates that after APPJ treatment, the amount of oxygen increased from 26.7 to 44.3 at%, whereas the fluorine content decreased significantly from 33.9 to 4.8 at%, and the fluorine to carbon ratio varied from 1.75 to 0.20. The high-resolution XPS data for C 1s and O 1s are shown in Fig. 2*d*. C 1s peaks were decomposed into six components corresponding to C–Si (283.8 eV), C–C/C–H (284.6 eV), –CO (286.1 eV), –COO (288.9 eV), $–CF_2$ (291.1 eV) and $–CF_3$ (293.7 eV), as shown in the upper row of Fig. 2*d*, which indicated that the $–CF_2$ and $–CF_3$ species significantly decreased after APPJ treatment,

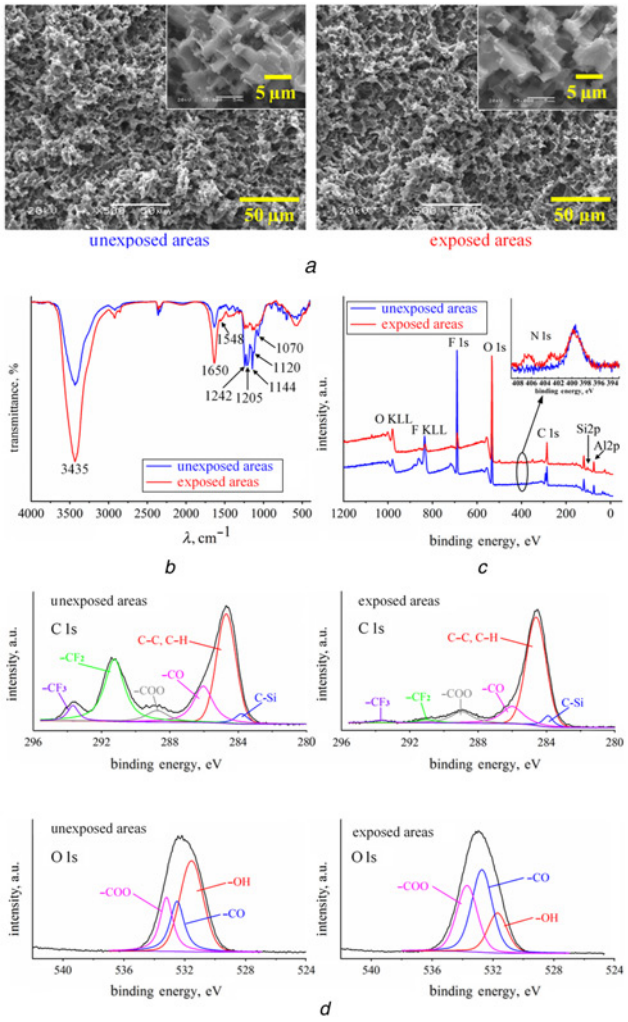

Figure 2 *Surface morphologies and chemical compositions analysis of unexposed and exposed areas on superhydrophobic aluminium surfaces during APPJ treatment*
a SEM images
b FTIR spectrum
c XPS spectrum
d High-resolution XPS spectrum for C 1s (upper two graphs) and O 1s (lower two graphs)

doi: 10.1049/mnl.2014.0590

whereas the O 1s XPS spectrum (lower row, Fig. 2*d*), which were resolved into –OH (531.6 eV), –CO (532.6 eV) and –COO (533.4 eV), indicated that the content of –CO and –COO species increased after APPJ treatment.

As shown in the XPS spectrum in Fig. 2*c*, there exists a little (~1 at%) nitrogen on the areas unexposed and exposed to APPJ. The observed N 1s peak at 399.5 eV is probably associated with nitrogen contaminants like C–N, which was not detectable in the C 1s spectra because of the low nitrogen concentrations and the fact that the C–N binding energy does not differ significantly from the C–O bonds [33]. The peaks at 403.1 and 407.1 eV after nitrogen APPJ treatment may be attributed to the adsorbed NO and N_2O on aluminium substrates [33, 34].

The metastable states of nitrogen [e.g. $N_2(A)$ and $N_2(a')$] are created during the nitrogen discharge by direct electron impact excitation from the molecular ground state, and they would take part in the downstream kinetics as well as in surface interactions [35]. Moreover, as the OES between 230 and 800 nm depicted in Fig. 3 shows, the nitrogen APPJ downstream contains various reactive radicals such as NO, OH and atomic oxygen, which indicates that the APPJ may offer highly active plasma chemistry and these radicals can play important roles in plasma–surface interactions applications. Note that the metastable nitrogen energy state is about 6.2 eV above the ground state, which is high enough to break the C–C (~3.8 eV) and C–F bonds (~4.5 eV). Therefore, under exposure of the APPJ, the C–F bonds of the FAS chains on the superhydrophobic aluminium surface were broken, OH and O are subsequently incorporated to oxidise the alkyl chains absorbed on the surface, and various C–O bonds were formed simultaneously through the APPJ downstream chemistry. As a result, a large amount of the low surface energy fluorine-containing functional groups (e.g. $–CF_2$ and $–CF_3$) were removed. The formed oxygen-containing functional groups (e.g. –CO and –COO) substantially improved the hydrophilic properties of the APPJ-treated areas. Therefore, the transition from superhydrophobicity to superhydrophilicity is because of the decrease of hydrophobic fluorine-containing functional groups and the increase of the hydrophilic oxygen-containing functional groups.

Fig. 4*a* shows the influence of APPJ treatment time on the wettability of the aluminium surface. Upon nitrogen APPJ treatment, the wettability of the superhydrophobic aluminium surface changed dramatically. The WCA decreased from 159° to 13° after APPJ treatment for 30 s and then slowly decreased further with increasing treatment time. After APPJ treatment for more than 45 s, the WCA was found to be less than 5°, that is the aluminium surface switched from superhydrophobic to superhydrophilic. It is noteworthy that the superhydrophilic surfaces created by APPJ treatment can recover to be superhydrophobic after being immersed in the re-prepared 1 wt% FAS-ethanol solution for 2 min. We supposed that the APPJ-treated area was covered by the low surface energy FAS again upon immersing in FAS-ethanol solution [36]. Fig. 4*b* shows the cycles of reversible superhydrophobicity and

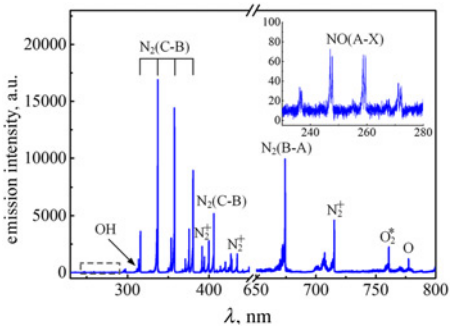

Figure 3 *Optical emission spectra of nitrogen APPJ downstream*

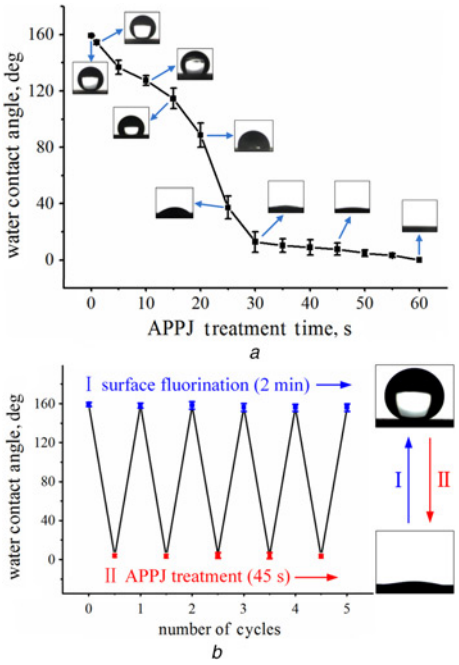

Figure 4 *Relationship between APPJ treatment time and WCA of surface and wettability transformation*
a Relationship between APPJ treatment time and WCA of surface
b Cycles of reversible superhydrophobicity and superhydrophilicity transformation by alternating between APPJ treatment and surface fluorination

superhydrophilicity transformation of the aluminium plates obtained by alternating between APPJ treatment and surface fluorination. As a whole, the switchable wettability transition was performed for five cycles, and the WCAs still reached more than 150° after the fluroalkylsilane treatment. The reversible wettability transition only took 3 min, which in principle enables rapid reversible hydrophilic patterning on superhydrophobic surfaces.

The APPJ treatment for surface patterning has good versatility. Wettability contrast patterns can also be easily and directly constructed on other metal substrates besides aluminium. Figs. 5*a–c* show, respectively, the snowflake-like pattern on the superhydrophobic titanium surface, the DUT (Dalian University of Technology) pattern on the superhydrophobic zinc surface and the hydrophilic microchannel on the superhydrophobic copper surface, which were all created by masked APPJ scanning exposure and dyed by food colouring. Therefore, combined with scanning

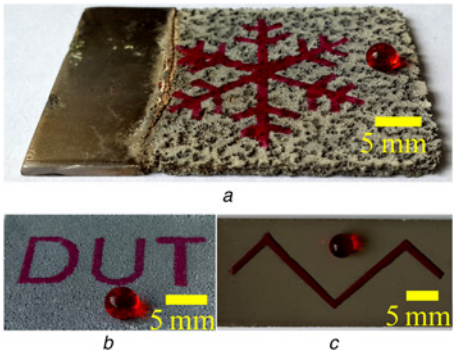

Figure 5 *Patterns created by APPJ selective exposure, visualised with food colouring*
a Snowflake on superhydrophobic titanium surface
b DUT on superhydrophobic zinc surface
c Microchannel on superhydrophobic copper surface

and mask technology, complex and large-area wettability contrast patterns on various superhydrophobic surfaces can be easily fabricated by APPJ exposure.

4. Conclusion: In summary, we have devised a fast and facile method to switch the wettability of superhydrophobic surfaces for patterning at atmospheric pressure and temperature, which may potentially be used for large-scale industrial processes as it does not require vacuum or high energy input. Then, hydrophilic patterns were fabricated on superhydrophobic surfaces by APPJ treatment. SEM results showed that the APPJ exposure had little influence on surface morphologies, whereas FTIR and XPS analyses demonstrated that the oxygen-containing groups introduced by the APPJ treatment accounted for the wettability contrast. Large-area and complex wettability contrast patterns can be constructed by the mask and scanning of the APPJ. Meanwhile, a reversible and high-efficiency wettability transition was achieved by alternating between APPJ treatment and surface fluorination, which enabled the surfaces to react and behave rapidly.

5. Acknowledgments: This work was financially supported by the National Natural Science Foundation of China (NSFC, grant nos. 51275072 and 51305060) and by the China Postdoctoral Science Foundation Funded Project (grant no. 2013M541223).

6 References

[1] Li D., Wang H.T.: 'Smart draw agents for emerging forward osmosis application', *J. Mater. Chem. A*, 2013, **1**, (45), pp. 14049–14060
[2] Cherenack K., Zysset C., Kinkeldei T., Munzenrieder N., Troster G.: 'Woven electronic fibers with sensing and display functions for smart textiles', *Adv. Mater.*, 2010, **22**, (45), pp. 5178–5182
[3] Zhai L., Berg M.C., Cebeci F.C., *ET AL.*: 'Patterned superhydrophobic surfaces: toward a synthetic mimic of the namib desert beetle', *Nano Lett.*, 2006, **6**, (6), pp. 1213–1217
[4] Chao S.H., Carlson R., Meldrum D.R.: 'Rapid fabrication of microchannels using microscale plasma activated templating (μPLAT) generated water molds', *Lab Chip*, 2007, **7**, (5), pp. 641–643
[5] Mumm F., van Helvoort A.T., Sikorski P.: 'Easy route to superhydrophobic copper-based wire-guided droplet microfluidic systems', *ACS Nano*, 2009, **3**, (9), pp. 2647–2652
[6] Her E.K., Ko T., Lee K., Oh K.H., Moon M.: 'Bioinspired steel surfaces with extreme wettability contrast', *Nanoscale*, 2012, **4**, (9), pp. 2900–2905
[7] Chatterjee A., Derby M.M., Peles Y., Jensen M.K.: 'Condensation heat transfer on patterned surfaces', *Int. J. Heat Mass Transf.*, 2013, **66**, pp. 889–897
[8] Seo J., Lee S., Lee J., Lee T.: 'Guided transport of water droplets on superhydrophobic-hydrophilic patterned Si nanowires', *ACS Appl. Mater. Interfaces*, 2011, **3**, (12), pp. 4722–4729
[9] Derby M.M., Chatterjee A., Peles Y., Jensen M.K.: 'Flow condensation heat transfer enhancement in a mini-channel with hydrophobic and hydrophilic patterns', *Int. J. Heat Mass Transf.*, 2014, **68**, pp. 151–160
[10] Ghosh A., Ganguly R., Schutzius T.M., Megaridis C.M.: 'Wettability patterning for high-rate, pumpless fluid transport on open, non-planar microfluidic platforms', *Lab Chip*, 2014, **14**, (9), pp. 1538–1550
[11] Sun R., Nakajima A., Fujishima A., Watanabe T., Hashimoto K.: 'Photoinduced surface wettability conversion of ZnO and TiO_2 thin films', *J. Mater. Chem. B*, 2001, **105**, (10), pp. 1984–1990
[12] Lim H.S., Kwak D., Lee D.Y., Lee S.G., Cho K.: 'UV-driven reversible switching of a roselike vanadium oxide film between superhydrophobicity and superhydrophilicity', *J. Am. Chem. Soc.*, 2007, **129**, (14), pp. 4128–4129
[13] Caputo G., Cortese B., Nobile C., *ET AL.*: 'Reversibly light-switchable wettability of hybrid organic/inorganic surfaces with dual micro-/nanoscale roughness', *Adv. Funct. Mater.*, 2009, **19**, (8), pp. 1149–1157
[14] Wang H., Duan J., Cheng Q.: 'Photocatalytically patterned TiO_2 arrays for on-plate selective enrichment of phosphopeptides and direct MALDI MS analysis', *Anal. Chem.*, 2011, **83**, (5), pp. 1624–1631
[15] Lee C., Cho H., Kim D., Hwang W.: 'Fabrication of patterned surfaces that exhibit variable wettability ranging from superhydrophobicity to high hydrophilicity by laser irradiation', *Appl. Surf. Sci.*, 2014, **288**, pp. 619–624
[16] Elsharkawy M., Schutzius T.M., Megaridis C.M.: 'Inkjet patterned superhydrophobic paper for open-air surface microfluidic devices', *Lab Chip*, 2014, **14**, (6), pp. 1168–1175
[17] Auad P., Ueda E., Levkin P.A.: 'Facile and multiple replication of superhydrophilic-superhydrophobic patterns using adhesive tape', *ACS Appl. Mater. Interfaces*, 2013, **5**, (16), pp. 8053–8057
[18] Tsougeni K., Papageorgiou D., Tserepi A., Gogolides E.: '"Smart" polymeric microfluidics fabricated by plasma processing: controlled wetting, capillary filling and hydrophobic valving', *Lab Chip*, 2010, **10**, (4), pp. 462–469
[19] Xin-Wei W., Yong-Xin S., Hao W.: 'Observation of nucleate boiling on a fine copper wire with superhydrophobic micropatterns', *Chin. Phys. Lett.*, 2012, **29**, (11), pp. 114702
[20] Meng H., Li G.Q.: 'Reversible switching transitions of stimuli-responsive shape changing polymers', *J. Mater. Chem. A*, 2013, **1**, (27), pp. 7838–7865
[21] Guo Y.D., Zhang G.K., Gan H.H., Zhang Y.L.: 'Micro/nano-structured $CaWO_4/Bi_2WO_6$ composite: synthesis, characterization and photocatalytic properties for degradation of organic contaminants', *Dalton Trans.*, 2012, **41**, (41), pp. 12697–12703
[22] Li L., Li L.H., Ramakrishnan S., *ET AL.*: 'Controlling wettability of boron nitride nanotube films and improved cell proliferation', *J. Phys. Chem. C*, 2012, **116**, (34), pp. 18334–18339
[23] Zhu X., Zhang Z., Men X., Yang J., Xu X., Zhou X.: 'Plasma/thermal-driven the rapid wettability transition on a copper surface', *Appl. Surf. Sci.*, 2011, **257**, (8), pp. 3753–3757
[24] West J., Michels A., Kittel S., Jacob P., Franzke J.: 'Microplasma writing for surface-directed millifluidics', *Lab Chip*, 2007, **7**, (8), pp. 981–983
[25] Xian Y.B., Lu X.P., Wu S.Q., Chu P.K., Pan Y.: 'Are all atmospheric pressure cold plasma jets electrically driven?', *Appl. Phys. Lett.*, 2012, **100**, (12), pp. 123702
[26] Lu Y., Song J.L., Liu X., Xu W.J., Sun J., Xing Y.J.: 'Loading capacity of a self-assembled superhydrophobic boat array fabricated via electrochemical method', *Micro Nano Lett.*, 2012, **7**, (8), pp. 786–789
[27] Song J., Xu W., Lu Y., Luo L., Liu X., Wei Z.: 'Fabrication technology of low-adhesive superhydrophobic and superamphiphobic surfaces based on electrochemical machining method', *J. Micro Nano Manuf.*, 2013, **1**, (2), pp. 21003
[28] Lu Y., Xu W., Song J., Liu X., Xing Y., Sun J.: 'Preparation of superhydrophobic titanium surfaces via electrochemical etching and fluorosilane modification', *Appl. Surf. Sci.*, 2012, **263**, pp. 297–301
[29] Yang X.L., Song J.L., Xu W.J., Liu X., Lu Y., Wang Y.P.: 'Anisotropic sliding of multiple-level biomimetic rice-leaf surfaces on aluminium substrates', *Micro Nano Lett.*, 2013, **8**, (11), pp. 801–804
[30] Hu K., Xu Q.X., Yang X.L.: 'Fabrication of superhydrophobic surfaces on copper substrates via brush plating technique', *Adv. Mater. Res.*, 2014, **834**, pp. 662–669
[31] Xu W., Huang S., Chen F., Song J., Liu X.: 'Diamond wear properties in cold plasma jet', *Diam. Relat. Mater.*, 2014, **48**, pp. 96–103
[32] Xia F., Jiang L.: 'Bio-inspired, smart, multiscale interfacial materials', *Adv. Mater.*, 2008, **20**, (15), pp. 2842–2858
[33] Panousis E., Clement F., Loiseau J.F., *ET AL.*: 'Titanium alloy surface treatment using an atmospheric plasma jet in nitrogen pulsed discharge conditions', *Surf. Coat. Tech.*, 2007, **201**, (16), pp. 7292–7302
[34] Pashutski A., Folman M.: 'Low-temperature XPS studies of NO and N_2O adsorption on Al(100)', *Surf. Sci.*, 1989, **216**, (3), pp. 395–408
[35] Chiang M.H., Liao K.C., Lin I.M., *ET AL.*: 'Effects of oxygen addition and treating distance on surface cleaning of ITO glass by a non-equilibrium nitrogen atmospheric-pressure plasma jet', *Plasma Chem. Plasma Process.*, 2010, **30**, (5), pp. 553–563
[36] Zhu X., Zhang Z., Xu X., *ET AL.*: 'Rapid control of switchable oil wettability and adhesion on the copper substrate', *Langmuir*, 2011, **27**, (23), pp. 14508–14513

doi: 10.1049/mnl.2014.0590